OPTOELECTRONICS AND ADVANCED MATERIALS – RAPID COMMUNICATIONS Vol. 1, No. 7, July 2007, p. 322 - 328

Comparative study of structural and optical properties of thermally evaporated and pulsed laser ablated CdSe thin films

A. M. A. EL-BARRY*, M. M. EL- NAHASS, A. A. ATTA
Thin film laboratory, Physics Department, Faculty of Education, Ain Shams University, Cairo, Egypt

A comparison, of some structural and optical properties for pulsed laser ablated (PLA) and thermally evaporated (TE) CdSe thin films, is given. The stoichiometry of the prepared films is checked by energy dispersive X-ray spectroscopy (EDX). Electron microscope data indicate the polycrystalline nature of the films with hexagonal structure. The degree of crystallinity is improved in PLA films. Some optical parameters for the two groups of CdSe films were compared over a wide range of wavelength (~ 200 - 2500 nm) at room temperature. The analysis of the data indicates that the dispersion parameters are affected by the technique of preparation more than the absorption parameters.

(Received March 13, 2007; accepted June 26, 2007)

Keywords: CdSe thin film, Laser ablation technique, Optical parameters

1. Introduction

The II-VI compound semiconductors are well known for application in a wide range of optoelectronic devices [1] and other applications [2]. There has been strong interest in the heteroepitaxially growth of good quality II-VI compound semiconductors on III-V compound semiconductors, especially on GaAs and InP because high quality commercial single crystalline wafers are available. Several techniques have been reported, such as e-beam evaporation [3], plasma sputtering [4], hot-wall epitaxy [5], metal-organic chemical vapor deposition [6], and molecular beam epitaxy (MBE) [7]. Pulsed laser ablation (PLA) has been used successfully to grow many different materials [8]. The PLA process can be divided into (at least) three steps: laser-target interaction, plume expansion and film deposition. Each process is highly material dependent as well as it depends on experimental parameters such as laser wavelength, pulse width, substrate type and temperature, and deposition geometry. The time scales involved in the three steps process are very different. Typically, the laser - target interactions occur within nanoseconds, whereas the plume expansion in the vacuum takes place within microseconds. Depending on experimental conditions, the film growth process following a laser pulse can continue to develop until the next laser pulse occurs milliseconds later. When a pulsed laser interacts with a target material, the process is often referred to as "laser ablation". Here "ablation" covers a variety of processes that occur during the interaction such as absorption, surface melting and vaporization, ejection of particles, and plasma formation and expansion. As indicated above, a variety of different interactions is involved in a laser ablation process. Not only the interaction between the laser and the target has to be considered, but also laser vapor, vapor-target, laser-plasma and plasma-target interactions play a role [8]. This technique is fully compatible with MBE sources in an ultrahigh vacuum environment. Single-crystal semiconductor epitaxial thin films have been made by this so-called "laser-MBE" technique [8]. The focused pulsed laser beam produces such a rapid temperature rise on the target, that the stoichiometry of the target is maintained in the growing film [9].This is thought to be a way to reduce group VI vacancies, which is the main source of the trouble of some native doping in II-VI compounds. High energy atoms and ions in the laser-induced plasma plume create a higher surface mobility, which makes it possible to grow high quality films at a relatively low substrate temperature [9]. Superlattice or multi-layer devices can be easily fabricated by PLA because of its flexibility in using multiple targets. The absence of a high temperature heater in the source region eliminates the necessity of expensive and complicated liquid nitrogen cooling [10]. CdSe is an important member of II-VI group of binary compounds. It has a direct intrinsic band gap of 1.74 eV that makes it an interesting material for various applications. The material has been grown in bulk single crystalline form and has been used as an efficient photo-detector [11]. Brient and Cappelletti [12] showed that compared to single source thermal evaporation, laser ablation preserves starting stoichiometry in the resulting thin films.

The present paper reports a simple study carried out for structural and optical properties of CdSe thin films, prepared by both thermally evaporation and laser ablation techniques. The optical results for the films prepared by these two techniques were compared for the first time.

2. Experimental details

Cadmium selenide thin films were prepared by two techniques; thermal evaporation (TE) and PLA of a stoichiometric powder of CdSe (chemical purity 99.999 %,

Balzer comp.). The TE films were deposited onto pre-cleaned quartz substrates, using a high vacuum coating unit (Edward type E 306A, England). The films were vacuum deposited from a quartz crucible source heated by a tungsten coil in a vacuum of 10^{-4} Pa during deposition. The substrate was kept at room temperature. The deposition rate was maintained at a rate of ~ 25 Å/s using a quartz crystal thickness monitor (Model FTM4, Edwards Co., England). The thicknesses of the films, were ~105 and ~296 nm. The second group of CdSe thin films was prepared by PLA technique, where the PLA apparatus is similar to that described by A. A. Alla [13]. The laser ablation deposition system used for thin films preparation consists of evaporation source and deposition chamber. The evaporation source is a Nd:YAG laser (Model PL-7010, CA 95051), with a fundamental wavelength 1064 nm. It is operated with a repetition rate of 10 Hz, maximum pulse energy of 800 mJ and pulse duration of 7 ns. The laser beam is then guided at right angle to the target through an optical collimating lens (focal length = 15 cm) and chamber quartz window. A schematic view of the film deposition setup is shown in Fig. 1. The film deposition took place in a vacuum chamber held at the pressure ~ 10^{-4} Pa. CdSe target, placed in a rotating target holder, was irradiated with infra-red (IR) laser pulse. Thereby, ablated target material was deposited on quartz substrates placed 60 mm apart from the target surface.

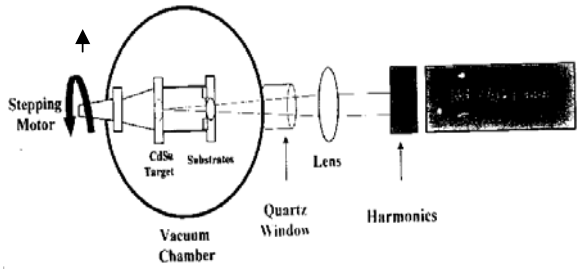

Fig. 1. The schematic diagram of pulsed laser deposition system [13].

The growth microstructure of CdSe thin films has been investigated using the diffraction technique. The films have been imaged by a JEOL-100S electron microscope and recorded in the constant mode at 60 kV. The chemical composition of the obtained films was checked by energy dispersive X-ray (EDX) using scanning electron microscope (Joel 5400).

The transmittance T(λ) and the reflectance R(λ) of the films were measured at normal incidence in the spectral range (~ 200 - 2500 nm) using a double beam spectrophotometer (JASCO model V.570UV-VIS-NIR). The transmittance and the reflectance measurements were measured at room temperature.

Table 1.

	Atomic percentage %		
	Source	TE-CdSe film	PLA-CdSe film
^{48}Cd	50.00	46.19	49.62
^{34}Se	50.00	53.81	50.38
Total	100.00	100.00	100.00
Atomic ratio, $\frac{^{48}Cd}{^{34}Se}$	100.00	85.84	98.49

From the measuring values of T, R and thickness t, the values of the refractive index n, and the absorption index k, were computed by using computed program, comprising a modified bivariate search technique, based on minimizing $(\Delta T)^2$ and $(\Delta R)^2$ simultaneously, within the desired accuracy[14], where

$$(\Delta T)^2 = (T_{n,k} - T_{\exp})^2;\ (\Delta R)^2 = (R_{n,k} - R_{\exp})^2 \quad (1)$$

Where T_{exp} and R_{exp} are the experimental values of T and R respectively, while $T_{n,k}$ and $R_{n,k}$ are the calculated values of T and R.

3. Results and discussion

3. 1. Structural properties

The EDX spectra, of both TE-CdSe thin film (~ 296 nm) and PLA–CdSe thin film (~ 282 nm), are shown in Fig. 2, and the obtained atomic percentages are listed in Table 1. Even though the source material contain 50 % selenium and 50 % cadmium, we got selenium rich TE- film compared with, more stoichiometric, PLA–film. Generally, II-VI compounds undergo complete dissociation during evaporation and the films are grown by allowing the constituent vapors to react with each other at the substrate at elevated temperatures. For both TE and PLA –CdSe films, of thinner thickness (~55 nm), the electron diffraction was utilized to investigate the structural properties. Fig. 3 (a, b) exhibits the electron diffraction patterns, which have clear rings. Through this figure, one can observe that the number of the rings for PLA-CdSe film (see Fig. 3b) is higher than that for TE-film (Fig. 3a). Firstly, the presence of the rings indicates the polycrystalline nature of the two films, regardless the preparation technique. Secondly, the crystallinity for PLA-film is higher than that for TE-CdSe film. The relation between ring's radius (r) and the spacing of the crystal planes (d_{hkl}) with Miller indices hkl, is given by: $\{d_{hkl} = L\lambda/(r_{hkl})\}$ [15], where Lλ (~53.8 nm) is known as the cammera constant. The ring patterns could be indexed on the basis of polycrystalline hexagonal structure [ICDD Card; No. 77-2307]. Ring diameter and the interplanar spacing, d_{hkl} for different hkl reflections for TE and PLA-CdSe films are listed in Table 2.

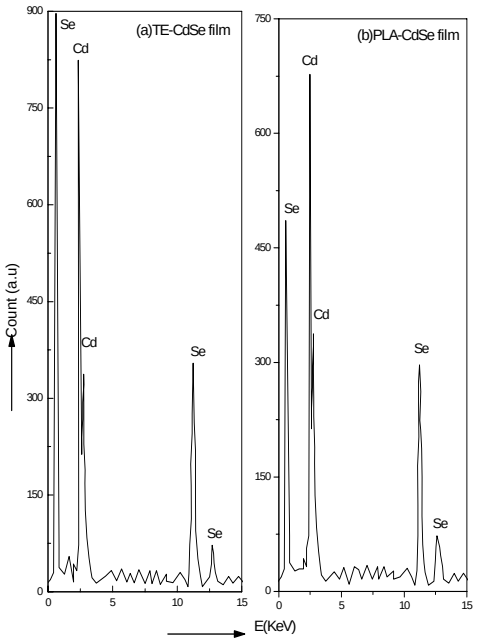

Fig. 2. Energy dispersive X-ray (EDX) spectroscopy for a) thermally evaporated (TE) CdSe thin film, with 296 nm thickness and b) pulsed laser ablated (PLA) CdSe thin film, with 282 nm thickness.

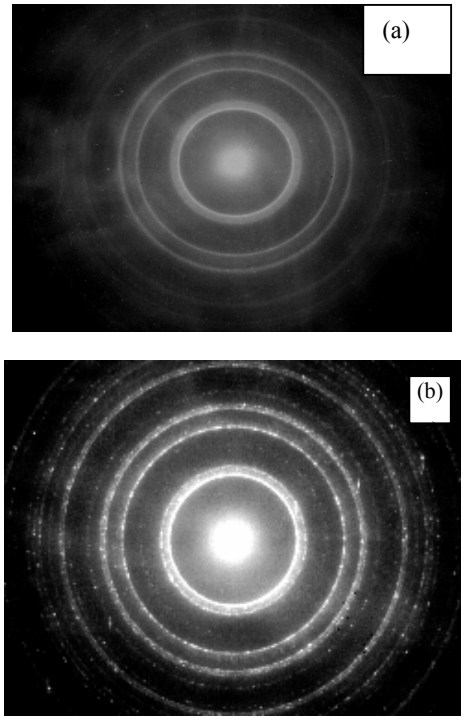

Fig. 3. Diffraction electron microscope (DEM) spectroscopy for a) thermally evaporated (TE) CdSe thin film and b) pulsed laser ablated (PLA) CdSe thin film (with ~ 55 nm thickness).

Table 2.

ICDD Card No,77-2307		TE-CdSe		PLA-CdSe	
d_{hkl}(Å)	hkl	r(nm)	d_{hkl}(Å)	r(nm)	d_{hkl}(Å)
3.723	100	1.423	3.78	1.446	3.72
3.505	002	-	-	-	-
3.288	101	1.7	3.165	1.6402	3.28
2.552	102	2.11	2.55	2.108	2.552
2.1492	110	2.55	2.11	2.5	2.152
1.979	103	--	-	-	-
1.862	106	-	-	2.9	1.855
1.832	112	-	-	2.95	1.823
1.799	201	3.00	1.793	2.99	1.799
1.7525	004	-	-	3.05	1.764
1.644	202	3.35	1.606	3.35	1.606
1.586	104	-	-	3.39	1.587
1.456	203	-	-	-	-
1.4071	210	-	-	3.823	1.4073
1.3796	211	3.9	1.379	3.875	1.388
1.3582	114	-	-	3.99	1.345
1.321	105	-	-	-	-
1.3058	212	-	-	4.12	1.306
1.276	204	-	-	-	-
1.241	300	4.34	1.24	4.34	1.2396
1.2054	213	-	-	4.46	1.206
1.1698	302	4.56	1.18	4.59	1.172
1.1683	006	-	-	4.719	1.14
1.1199	205	4.75	1.133	4.808	1.119
1.1147	106	-	-	4.83	1.114
1.097	214	5.35	1.006	5.17	1.04

3.2. Optical properties

The optical transmission and reflection spectra of both TE and PLA – CdSe films were recorded at room temperature in the spectral range 200 – 2500 nm, which covers the fundamental optical absorption edge and the inter-band transition regions of the semiconductor. Because of the wide differences in the values of the refractive index (n) of the semiconductor thin film (n ~ 3) and that of the quartz substrate (n~1.47), interference fringes appeared in all the transmission and reflection spectra.

Typical sets of transmission and reflection spectra of CdSe thin films, with different thickness obtained by both TE and PLA techniques, were used to determine the optical constants. We tried to study the effect of each technique on the optical properties.

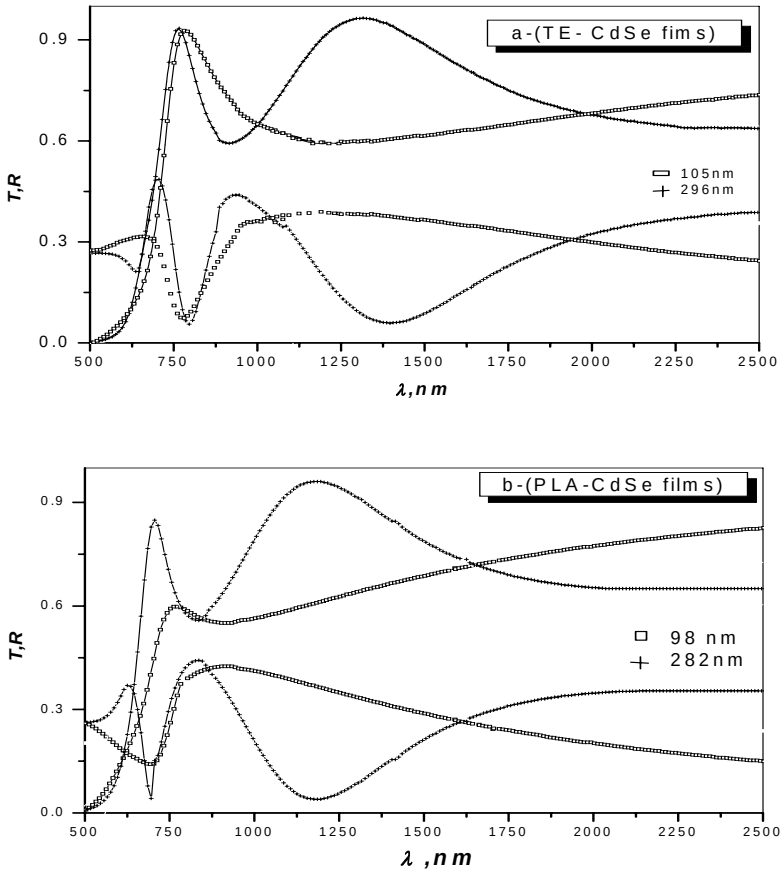

Fig. 4. Transmission, T and Reflection, R as a function of the wavelength, λ of the incident light for a) thermally evaporated (TE) CdSe thin films and b) pulsed laser ablated (PLA) CdSe thin films with different thickness.

Both T (λ) and R (λ) are represented in Fig. 4 (a,b). It could be noted that at longer wavelength (λ > 700 nm) the films became, nearly transparent, where T+R ≈ 1. Both the refractive index (n) and the absorption index (k), were determined at a given wavelength, using a computer program, based on Murmann's exact equation [16]. The curves of both the refractive index, n (λ) and the absorption index, k (λ) for CdSe films, are illustrated in Fig. 5. The values of n (λ) and k (λ), shown in this figure represent the mean values of n and k, for films of different thickness (98- 296 nm). The curves of the refractive index, for both TE and PLA films, can be divided into two regions. In the lower wavelength region, the refractive index, n has an anomalous behaviour until a critical wavelength, λ_c. The coverted dispersion index behaves normally. The increase of the refractive index for TE-CdSe films in comparison with that for PLA-CdSe films, may be due to the increased polarizability associated with the decrease of the stoichiometry [17].

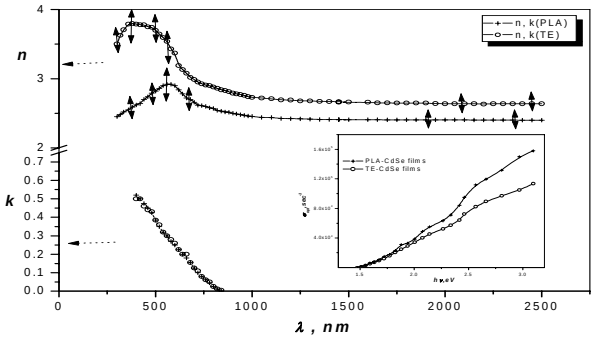

Fig. 5. The refractive index, n(λ) and the absorption index, k(λ) as a function of the wavelength, (λ) of the incident light for thermally evaporated (TE) CdSe thin films, and pulsed laser ablated (PLA) CdSe thin films, the inset figure: the optical conductivity, σ_{opt} as a function of the photon energy, hν, for thermally evaporated (TE) and pulsed laser ablated (PLA) CdSe thin films.

3.2.1. Absorption coefficient and energy gap determination

The determination of the optical constants, n and k, gave us the ability to study the absorption coefficient (α) for both TE and PLA – CdSe films, which can be calculated using the well– known relation, $\alpha = \frac{4\Pi k}{\lambda}$. In the spectral region of strong absorption ($\alpha > 10^4$) cm^{-1} the optical gap, E_g^{opt} is defined according to the following relation[18]

$$\alpha = A\frac{\left(h\upsilon - E_g{}^{opt}\right)^r}{h\upsilon} \qquad (2)$$

where A is a constant, hν is the photon energy, E_g^{opt} is the optical energy gap of the material and r is a number which characterizes the type of transition process [r has the value $\frac{1}{2}$ for the direct allowed transitions, $\frac{3}{2}$ for the direct forbidden transitions and has the value 2 for indirect allowed transitions while 3 for the indirect forbidden transitions]. The usual method for the determination of the value of $E_g{}^{opt}$ involves plotting graph of $(\alpha h\upsilon)^{1/r}$ vs. h*ν*. The data were analyzed according to the different types of transitions where, only the allowed direct transition is the most suitable for the obtained data. Fig. 6 illustrates $(\alpha h\nu)^2$ vs. h*ν*. Extrapolation of the linear dependence to the abscissa yields the corresponding allowed direct band width, $E_{g1}{}^{opt}$ ≈ 1.7 eV, for PLA films and ≈ 1.69 eV for TE films, indicating that CdSe thin films exhibit direct allowed transitions, in agreement with Shreckanthan et al. [32]. Moreover, the graphical representation of $(\alpha h\nu^2)$ vs. (h*ν*) for higher photon energy > 2 eV, yields another straight line, indicating another direct optical transition with energies, $E_{g2}{}^{opt}$ ≈ 2.12 eV for PLA films and ≈ 2.1 eV for TE films. The second transition is in agreement with that predicated by Thutupalli and Tomlin [19] who showed that the first direct transition to be clearly enough and evidently the second transitions occurs at about 2 eV or a little higher. Such behaviour is explained on the base of an energetic bands model [20-21] considering the spin orbit splitting. Thus, the splitting of the valence band, $\Delta_{so} \approx 0.41$, compared with 0.42 eV [20].

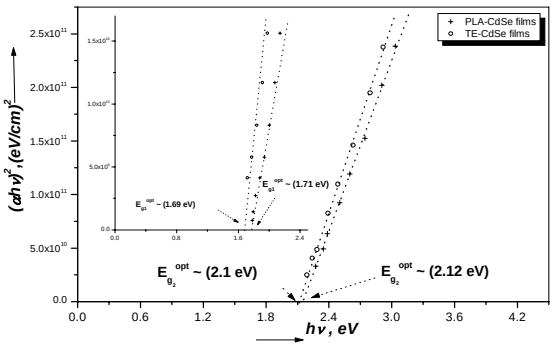

Fig. 6. $(\alpha h\nu)^2$ as a function of the photon energy, hν for thermal evaporated (TE) and pulsed laser ablated (PLA) CdSe thin films.

3.2.2. Dispersion Behaviour of the refractive index

An interesting model, describing the n dispersion curve, was Wemple-Di-Domenico [22] and Wemple [23] dispersion model. This model is represented by the following relation:

$$\frac{1}{n^2-1} = \frac{E_0}{E_d} - \frac{(h\upsilon)^2}{E_0 E_d} \qquad (3)$$

where EO and E_d are two parameters connected to the optical properties of the material. They are known as the single oscillator energy (E_0) and (E_d). The average strength of inter-band optical transition. Plotting $\frac{1}{n^2-1}$ against $(h\upsilon)^2$ allowed us to determine the oscillator parameters by fitting a straight line to the points, see Fig. 7. The values of E_0, E_d, the single oscillator strength, f ($E_d = \frac{f}{E_0}$) and the high frequency dielectric constant, ε_∞ ($\varepsilon_\infty = n^2 at \lambda^2 = 0$) can be determined directly from the slope and the intercept on the vertical axis. The straight line equations corresponding to the least- squares fit are, $\frac{1}{n^2-1}$ = 0.174 – 0.109 $(h\upsilon)^2$ for TE-CdSe films and $\frac{1}{n^2-1}$ = 0.2098 – 0.1$(h\upsilon)^2$ for PLA- CdSe films. As was found by Tanaka [24], the first approximated value of the optical band gap, E_g^{opt}, can be derived according to the expression $E_g^{opt} \approx E_0/2$. The values of the first optical gaps ratio ($\frac{E_0}{E_{g1}{}^{opt}}$) and the second optical gaps ratio ($\frac{E_0}{E_{g2}{}^{opt}}$), for CdSe films, are listed in Table 3. Table 3 lists the values of the single – oscillator parameters, compared with those reported before [19-20, 25]. Regarding the equation which correlated the optical constants, and the carrier concentration N, the lattice

optical dielectric constants ε_L can be directly obtained as follows [26];

$$n^2 = \varepsilon_l - \frac{e^2 N \lambda^2}{4\Pi^2 \varepsilon_0 c^2 m^*} = \varepsilon_l - B\lambda^2 \qquad (4)$$

where $B = \frac{e^2 N}{4\Pi^2 \varepsilon_0 c^2 m^*}$ and ε_l. is the lattice dielectric constant Plotting n^2, on the ordinates vs. λ^2 on the abscissa ,two straight lines are obtained (see the inset of Fig. 7). Taking into consideration Eq. 4 and the inset of Fig. 7, the values of both ε_l and $\frac{N}{m^*}$ were determined from the extrapolation of these plots to $\lambda^2 = 0$. Depending on the reported value of $N \simeq 1.2 \times 10^{24}/m^3$ [27], m* was found to be ~ 0.17 m_e for TE films while ~ 0.2 m_e for PLA CdSe films compared with 0.2 m_e [28]. The values of the lattice dielectric constant, ε_L are ~ 6.59 and ~ 6.8 (for PLA and TE films, respectively) compared with 6.4 [27] and 6.2 [29]. The difference between the values of ε_L and ε_∞ may be ascribed to the free carrier absorption. Also, one can observe that this difference is slightly higher for TE films and this may be attributed to the excess of Se.

Table 3.

Optical parameters	The present work		References
	TE- CdSe films	PLA- CdSe films	
E_{g1}(eV)	1.69	1.71	1.74[19]
E_{g2}(eV)	2.1	2.12	2.10[20]
Δ_{so} (eV)	0.41	0.41	0.42[25]
$\frac{E_0}{E_{g1}}$	2.34	2.678	
$\frac{E_0}{E_{g2}}$	1.9	2.16	
E_0 (eV	3.99	4.58	4.00[25]
E_d(eV	22.99	21.82	20.4[25]
f $(eV)^2$	91.74	99.94	81.6[25]
ε_{oo}	6.76	6.276	6.40[27]
ε_l	6.80	6.59	6.20[29]
$\frac{N}{m^*}, \frac{1}{kg.m^3}$	6.80×10^{51}	$5.45. \times 10^{51}$	
m *	0.17	0.20	0.20[28]
μ, $\frac{m^2}{V.s}$ at (R.T and 3 eV)	6.25	8.33	7.4 [27] at room temperature

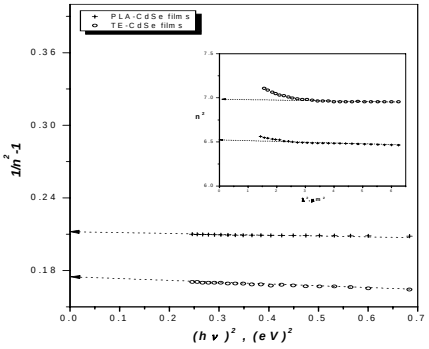

Fig. 7 . $\frac{1}{n^2-1}$ as a function of the square of the photon energy $(hv)^2$ of the incident light, for thermal evaporated (TE) CdSe thin films, and pulsed laser ablated (PLA) CdSe thin films, the inset figure: the square of the refractive index, n^2 as a function of the square of the wavelength, λ^2 of the incident light for thermal evaporated (TE) and pulsed laser ablated (PLA) CdSe thin film in the nonabsorbing region.

Another significant parameter, which can be extracted from the reflection data is the relaxation time τ (ω).This parameter, which represents the time of single oscillation in the potential well, can be calculated along the studied spectral range using the following formula [30].

$$\tau(\omega) = \frac{\varepsilon_\infty - \varepsilon_2}{\omega \varepsilon_2} \qquad (5)$$

where τ is the dielectric relaxation time and ω is the angular frequancy. The calculated values of the relaxation time represented a rapid decreasing in its value from (820 ± 0.09) fs at lower photon energy ~ 0.5 eV, to ~ (10.5 ± 0.075) fs for TE- films, while it reached to ~ (19.8 ± 0.034) fs for PLA films, at higher photon energy ~ 6.2 eV. The value of τ for PLA- films appeared to be higher than that for TE-film at higher photon energy. This may be due to a decrease in the scattering centers.

The determination of the optical constants, n and k, gave us the possibility to study the spectral dependence of the optical conductivity, σ_{opt}, at room temperature according to the following relation [31].

$$\sigma_{opt} = 2nk\varepsilon_0\omega \qquad (6)$$

where ε_o is the permittivity of free space. The inset of Fig. 5 shows that the PLA- technique leads to a slight increase

in the optical conductivity compared with TE- technique. The free carrier mobility in thin films, μ, was calculated from the experimental values of σ_{opt} according to the relation, $\sigma = \mu Ne$, [31]. The values of the effective carrier concentrations and the mobility can be regarded only as rough estimation (at room temperature and at 3eV, as an example, see Table 3). On the other hand II–VI compounds dissociate upon evaporation in vacuum, and films prepared by this technique actually mean the reconstitution of the vapour elements [32]. Thus CdSe films prepared by PLA- technique are of better stoichiometry. Nevertheless, it is seen that the values of the average value of the mobility of the free carriers through the thermally evaporated films is lower than that in PLA-films. This may be due to the presence of defect states in the forbidden gap [12], where it was found that vacuum backing of CdSe, containing either excess of Cd or of Se, determines a change of the stoichiometry of the compound and therefore an increase of the concentration of scattering centers [33].

4. Conclusions

For two groups of CdSe films, fabricated by both thermally evaporation (TE) and pulsed laser ablation (PLA) techniques, the following results were obtained.

1-The analysis of EDX-data showed that the deposited PLA-film is homogenous and nearly stoichiometric. The electron microscopy revealed the polycrystalline nature of the hexagonal phase and the crystallinity is improved for PLA-CdSe films.

2-The dispersion parameters seem likely to be dependent on the technique of preparation, where they are higher for thermally evaporated films than those for pulsed laser ablated films. This behaviour may be due to a decreasing in the scattering centers in PLA-films at higher energy.

3- There are two allowed direct transitions, regardless the technique of preparation, $E_{g\,1}^{opt} \approx 1.71$eV, for PLA films and 1.69 eV for TE film and $E_{g\,2}^{opt} \approx 2.12$ eV for PLA films and 2.1 eV for TE films. Such behaviour has been explained by considering the spin orbit splitting, $\Delta_{so} \approx 0.41$.

Acknowledgement

The authors are grateful to A. S. G. A. Alla, member of Laser Systems Department, National Institute of Laser Enhanced Science, Cairo University, Egypt.

References

[1] J. Britt, C. Ferekides, Appl. Phys Lett. **62**, 2851 1993).
[2] W. P. Shen, H. S. Kwok, Appl. Phys Lett. **65**(17), 2162 (1994).
[3] F. M. Livingstone, W. Duncan, T. Baird, J. Appl. Phys. **48**, 3807 (1977).
[4] I. Martil, G. Gouzalez-Diaz, F. Sanchez-Quesada, J. Vac. Sci. Technol. **A2**, 1491 (1984).
[5] J. Humenberger, G. Linnert, K. Lischka, Thin Solid Films **121**, 75 (1984).
[6] Y. Endoh, T. Kawakami, T. Taguchi, A. Hiraki, Jpn. J .Appl. Phys. **27**, L2, 199 (1988).
[7] R. M. Park, M. B. Troffer, C. M. Rouleau, J. M. DePuydt, M. A. Haase, Appl. Phys. Lett. **57**, 2127 (1990).
[8] D. B. Chrisey, G .K.Hulber, Plused Laser Deposition of Thin Film, (Wily, New York), 1994.
[9] J. T. Cheung, H. Sankur, CRC Crit Rev. Solid State Mater. Sci. **15**, 63 (1988).
[10] J. A. Greer, J. Vac. Sci. Technol. **A10**, 1821 (1992).
[11] K. N. Shreekanthan, B. N. Rajendra, V. B. Kastruri, G. K. Shivakumary, Cryst. Res. Technol. **38**(1), 30 (2003).
[12] C. R. Brient, R. L. Cappelletti, J. Mater. Res. **5**(3), 511 (1996).
[13] A. S. G. A. Alla, M. Sc. Thesis, Investigation of optical and electrical properties of laser deposited CdS thin films to be used in photoelectric applications, Cairo Univ., National Institute of Laser Enhanced Science, Laser systems department, 2004, p: 38-41.
[14] M. M. EL-Nahass, A. M. A. EL-Barry, A. A. Farag, S. Y. EL-Soly, Eur. Phy. J. AP. acceptance 19-1-2006.
[15] P. B. Hirsch, A. Howie, R. B. Nichloson, Electron Microscopy of Thin Crystals, Butter Worths, London (1950).
[16] H. Murmann, J. Phys. **101**, 643 (1936).
[17] M. M. EL- Nahass, M. B. EL-den, Optics & Laser Technolgy. **33**, 31 (2001).
[18] M. M. EL-Nahass, A. A. M. Farag, E. M. Ibrahim, S. Abd-El-Rahman, Vacuum, **72**, 453 (2004).
[19] K. N. Shreckanthan, B. V. Raj endra, V. B. Kastrui, G. K. Shivakumar, Cryst. Res. Technol. **38**(1), 30 (2003).
[20] G. K. M. Thutupalli, S. G. Tomlin, J. Phys D: Appl. Phys. **9**, 1634 (1976).
[21] A. Abd El- Mongy, Egypt. J. Sol. **27**(1), 111 (2004).
[22] S. H. Wemple, M. Didomenico, J. Phys. Rev. **B3**, 1338 (1971).
[23] S. H. Wemple, J. Phys Rev. **B7**, 3667 (1973).
[24] K. Tanaka, Thin Solid Films **66**, 271 (1980).
[25] S. H. Wemple, M. Di Domenico, phys Rev. lett. **23**, 20 (1969).
[26] M. M. EL-Nahass, M. B. EL-Den, H. E. A. EL-Sayed, A. M. A. EL-Barry, M. A. M. Seyam, J. Optoelectron. Adv. Mater. **8**(5), 1817 (2006).
[27] K. N. Sharma, K. Barua, J. phys D: Appl. Phys. **12**, 1729 (1979).
[28]Y. R. C. Kainthla, D. K. Pandya, K. L. Chopra. Solid state. Electronics **25**(1), 73 (1982).
[29] M. M. EL-Nahass, Z. EL-Gohary, H. S. Soliman, Optics & Laser Technology **35**, 523 (2003).
[30] K. L. Chopra,Thin Solid Phenomena, M. C. Green–Hill, New York (1969) p.721.
[31] M. Baleva,E. Goranova, V. Darakchieva, S. Kossionides, M. Kokosis, P. Jordanov, Vacuum **69**, 425 (2003).
[32] D. A. Cusano, physics and chemistry of II – VI compounds, Eds. M. Aven and J.S. prener (Amsterdam: North – Hollano (1967) P. 710.
[33] G. A. Somorjai, J. Phys Chem. Solids **24**, 175 (1963).

*Corresponding author: amall56@yahoo.com